MMSE Signal Detection for MIMO Systems based on Ordinary Differential Equation

Ayano Nakai-Kasai
Graduate School of Engineering
Nagoya Institute of Technology
Nagoya, Japan
nakai.ayano@nitech.ac.jp

Tadashi Wadayama
Graduate School of Engineering
Nagoya Institute of Technology
Nagoya, Japan
wadayama@nitech.ac.jp

Abstract—Motivated by emerging technologies for energy efficient analog computing and continuous-time processing, this paper proposes continuous-time minimum mean squared error estimation for multiple-input multiple-output (MIMO) systems based on an ordinary differential equation. Mean squared error (MSE) is a principal detection performance measure of estimation methods for MIMO systems. We derive an analytical MSE formula that indicates the MSE at any time. The MSE of the proposed method depends on a regularization parameter which affects the convergence property of the MSE. Furthermore, we extend the proposed method by using a time-dependent regularization parameter to achieve better convergence performance. Numerical experiments indicated excellent agreement with the theoretical values and improvement in the convergence performance owing to the use of the time-dependent parameter.

Index Terms—Ordinary differential equation, MIMO, MMSE estimation, analog computing

I. Introduction

In the next generation wireless communication systems, beyond 5G and 6G, massive connectivity should be achieved with ultra high speed and large capacity communication [1]. The number of mobile devices increases every year, and the traffic and computational loads at the base stations are becoming heavier. It has been pointed out that there remain various implementation challenges with regard to the fulfillment of the demand for large-scale signal processing in base stations of the next generation wireless network systems [2]. In particular, typical signal detection methods in multiple-input multiple-output (MIMO) systems such as zero-forcing and minimum mean squared error (MMSE) [3] detection methods depend on centralized processing at the base station and require a heavy computational burden for the matrix inversion computation, which requires, in general, a cubic time complexity. The significant amount of signal detection loads in a base station has become a major bottleneck in the implementation of the next generation systems [1]. Massive parallel computation with matrix inversion hardware [4] may be one of the solutions but it needs tremendous energy consumption. Therefore, there are strong demands to develop novel signal processing methods to achieve reasonable signal detection performance with high

energy efficiency. One possibility to ease the bottleneck would be to reconsider analog-domain signal processing.

Recently, in the field of deep learning (DL), analog-domain computation has regained researchers' attention mainly from the perspective of computational efficiency [5]–[7]. Analog optical computing such as a photonic chip-based neural network (NN) proposed in [8] also has several advantages such as high computational efficiency, scalability, and stability. One of the recent studies was a complex-valued NN on a photonic chip proposed by Zhang et al. [9]. In addition to this, the optical computation is expected to play an important role in solving large-scale problems such as combinatorial optimizations or probabilistic graphical models [10].

These works inspire us to exploit such analog-domain signal processing not only for deep neural networks but also for wireless communication networks. An analog computer is fundamentally composed of analog adders, multipliers, integrators, and other nonlinear devices, and it can simulate any linear/nonlinear ordinary differential equations (ODEs). If one can formulate a high-dimensional signal detection task as a continuous-time dynamical system, it can be implemented with analog devices, and we can expect that they will provide high energy efficiency.

Another advantage of continuous-time dynamical systems for a signal processing task is that they bring us an insight into the discrete-time algorithms for solving the task, which is a counterpart of the continuous system. Neural ODE [11] is an ODE including a NN, i.e, its dynamics can be learned from data. Any numerical method for solving neural ODEs such as the Euler method and the Runge-Kutta method can be used for discretizing a high-dimensional neural ODE. The correspondence between the continuous neural dynamical system and the discrete-time inference procedure opens a new way to understand the property of the discrete-time procedure.

In this paper, we revisit analog-domain computing as a tool for overcoming the computing bottleneck at the base station in wireless communications and explore new signal detection methods. We present a continuous-time MMSE signal detection method for MIMO systems, which is derived directly as a form of ODE without any matrix inversion computation. With the benefit of the ODE representation, we can obtain theoretical analyses of the ODE-based MMSE detection method for

MIMO signals. To the best of our knowledge, there are no directly relevant proposals and analyses in previous literature.

The main contributions of this paper are listed below:

1) We propose a continuous-time MMSE detection method for MIMO signals. The method includes a regularization parameter that controls convergence behavior of the estimation method. We show the stability of the proposed method.

2) We derive an analytical formula of mean squared error (MSE) in a closed form. The MSE is the principal performance measure of signal detection methods. The formula is based on the eigenvalue decomposition of the Gram matrix. From the MSE formula, we immediately derive the asymptotic MSE. These analyses enable us to track the quality of the estimation at any time instant.

3) We introduce a time-dependent regularization parameter to achieve improved convergence performance. We also derive an analytical MSE formula for the time-dependent system. Numerical experiments will show that the convergence performance is improved by optimizing the time-dependent regularization parameter.

Analog computing for high-dimensional signal processing is a developing technology from a hardware point of view, but we believe that the analysis of the proposed method is a meaningful step toward forthcoming analog-domain high dimensional signal processing in wireless communications.

II. PRELIMINARIES

A. Notations

In the rest of the paper, we use the following notations. The superscript $(\cdot)^{\mathrm{H}}$ denotes the Hermitian transpose. The zero vector and identity matrix are represented as $\mathbf{0}$ and $\boldsymbol{I}$, respectively. ℓ_2-norm is $\|\cdot\|$. The complex circularly symmetric Gaussian distribution $\mathcal{CN}(\mathbf{0}, \boldsymbol{\Sigma})$ has mean vector $\mathbf{0}$ and covariance matrix $\boldsymbol{\Sigma}$. The expectation and trace operators are $\mathbb{E}[\cdot]$ and $\mathrm{Tr}[\cdot]$, respectively. The diagonal matrix is given by $\mathrm{diag}[\ldots]$ with the diagonal elements shown in the square brackets.

B. System Model

In this paper, we consider the following received signal model:

$$\boldsymbol{y} = \boldsymbol{H}\boldsymbol{s} + \boldsymbol{w}, \tag{1}$$

where $\boldsymbol{y} \in \mathbb{C}^m$ is the received signal, $\boldsymbol{H} \in \mathbb{C}^{m \times n}$ is the channel matrix, $\boldsymbol{s} \in \mathbb{C}^n$ is the transmitted signal that follows $\mathcal{CN}(\mathbf{0}, \boldsymbol{I})$, and $\boldsymbol{w} \in \mathbb{C}^m$ is the measurement noise that follows $\mathcal{CN}(\mathbf{0}, \sigma^2\boldsymbol{I})$. In the following, the channel matrix $\boldsymbol{H}$ is assumed not to be a zero matrix.

A linear estimate $\hat{\boldsymbol{s}} := \boldsymbol{W}\boldsymbol{y}$ for MIMO systems is characterized by the matrix $\boldsymbol{W} \in \mathbb{C}^{n \times m}$, which is determined according to each estimation method. The matrix $\boldsymbol{W}$ for MMSE signal detection [3] can be obtained by minimizing the MSE given by $\mathbb{E}[\|\boldsymbol{W}\boldsymbol{y} - \boldsymbol{s}\|^2]$. The resulting MMSE estimate is derived as

$$\hat{\boldsymbol{s}} = \left(\boldsymbol{H}^{\mathrm{H}}\boldsymbol{H} + \sigma^2\boldsymbol{I}\right)^{-1}\boldsymbol{H}^{\mathrm{H}}\boldsymbol{y}. \tag{2}$$

III. MMSE ESTIMATION AS ODE

In the case of continuous-time systems, it is often difficult to calculate the inverse of a matrix [12], so that deriving the MMSE estimate (2) is not straightforward. This paper considers a gradient dynamical system for the MMSE estimation and describes the evolution of the estimate in continuous-time systems.

A function

$$f(\boldsymbol{x}) := \|\boldsymbol{y} - \boldsymbol{H}\boldsymbol{x}\|^2 + \eta\|\boldsymbol{x}\|^2, \tag{3}$$

where $\eta > 0$, can be regarded as the objective function for MMSE signal detection because the unique stationary point of $f(\boldsymbol{x})$ coincides with the MMSE estimate (2) when $\eta = \sigma^2$ [13]. The scalar value η in (3) behaves as a regularization parameter. The gradient vector of $f(\boldsymbol{x})$ is given by $\nabla f(\boldsymbol{x}) = (\boldsymbol{H}^{\mathrm{H}}\boldsymbol{H} + \eta\boldsymbol{I})\boldsymbol{x} - \boldsymbol{H}^{\mathrm{H}}\boldsymbol{y}$.

In this paper, we regard the objective function (3) as a potential function of a continuous-time gradient dynamical system. We then obtain an estimate, $\boldsymbol{x}(t)$, of the transmitted signal $\boldsymbol{s}$ at time $t \geq 0$ that evolves according to the ODE

$$\frac{d\boldsymbol{x}(t)}{dt} = -\nabla f(\boldsymbol{x}(t)) = -(\boldsymbol{H}^{\mathrm{H}}\boldsymbol{H} + \eta\boldsymbol{I})\boldsymbol{x}(t) + \boldsymbol{H}^{\mathrm{H}}\boldsymbol{y}. \tag{4}$$

We further assume the initial condition $\boldsymbol{x}(0) = \boldsymbol{H}^{\mathrm{H}}\boldsymbol{y}$. We name the proposed signal detection based on the ODE (4) Ordinary Differential Equation-based MMSE (ODE-MMSE) method.

A closed-form representation of the estimate $\boldsymbol{x}(t)$ can be derived by the solution for a first-order linear ODE with constant coefficients [14]. This gives an analytical insight into the ODE-MMSE method discussed in the next section.

Proposition 1: The estimate of ODE-MMSE method at time $t \geq 0$ that follows the ODE (4) is represented as a random vector depending on the transmitted signal vector $\boldsymbol{s}$ and the noise vector $\boldsymbol{w}$, and given by

$$\boldsymbol{x}(t) = (\boldsymbol{Q}(t) + \boldsymbol{R})(\boldsymbol{H}\boldsymbol{s} + \boldsymbol{w}), \tag{5}$$

where

$$\boldsymbol{Q}(t) := \exp\left(-(\boldsymbol{H}^{\mathrm{H}}\boldsymbol{H} + \eta\boldsymbol{I})t\right)\left(\boldsymbol{I} - (\boldsymbol{H}^{\mathrm{H}}\boldsymbol{H} + \eta\boldsymbol{I})^{-1}\right)\boldsymbol{H}^{\mathrm{H}}$$

and $\boldsymbol{R} := (\boldsymbol{H}^{\mathrm{H}}\boldsymbol{H} + \eta\boldsymbol{I})^{-1}\boldsymbol{H}^{\mathrm{H}}$.

Proof: An equilibrium point $\boldsymbol{x}^*$ of the ODE (4) can be obtained as the solution of the equation $\frac{d\boldsymbol{x}(t)}{dt} = 0$. This is given by $\boldsymbol{x}^* = (\boldsymbol{H}^{\mathrm{H}}\boldsymbol{H} + \eta\boldsymbol{I})^{-1}\boldsymbol{H}^{\mathrm{H}}\boldsymbol{y}$. The equilibrium point is unique because the potential function (3) is strictly convex. We define the residual error vector between $\boldsymbol{x}(t)$ and the equilibrium point as $\boldsymbol{e}(t) := \boldsymbol{x}(t) - \boldsymbol{x}^*$, and then the ODE (4) can be replaced with

$$\frac{d\boldsymbol{e}(t)}{dt} = \frac{d\boldsymbol{x}(t)}{dt} = -(\boldsymbol{H}^{\mathrm{H}}\boldsymbol{H} + \eta\boldsymbol{I})\boldsymbol{e}(t). \tag{6}$$

This is the typical first-order linear ODE with constant coefficients and can be solved with a matrix exponential [14]. The solution is given by

$$\begin{aligned} \boldsymbol{e}(t) &= \exp\left(-(\boldsymbol{H}^{\mathrm{H}}\boldsymbol{H} + \eta\boldsymbol{I})t\right)\boldsymbol{e}(0) \\ &= \exp\left(-(\boldsymbol{H}^{\mathrm{H}}\boldsymbol{H} + \eta\boldsymbol{I})t\right)\left(\boldsymbol{I} - (\boldsymbol{H}^{\mathrm{H}}\boldsymbol{H} + \eta\boldsymbol{I})^{-1}\right)\boldsymbol{H}^{\mathrm{H}}\boldsymbol{y}. \end{aligned} \tag{7}$$

Therefore, the solution of (4) can be obtained by substituting (7) and (1) for $\boldsymbol{x}(t) = \boldsymbol{e}(t) + \boldsymbol{x}^*$, and by summarizing the terms of the equation. □

The stability of the system (6) can be evaluated via the eigenvalues of the matrix $\boldsymbol{A} := \boldsymbol{H}^{\mathrm{H}}\boldsymbol{H} + \eta\boldsymbol{I}$.

Proposition 2: The system (6) is stable.

Proof: From (6), the stability of the system depends on the Hermitian matrix $-\boldsymbol{A} = -(\boldsymbol{H}^{\mathrm{H}}\boldsymbol{H} + \eta\boldsymbol{I})$. The Hermitian matrix $\boldsymbol{H}^{\mathrm{H}}\boldsymbol{H}$ is positive semidefinite and the matrix $\eta\boldsymbol{I}$ is positive definite. The Hermitian matrix $-\boldsymbol{A}$ becomes negative definite so that it only has real and negative eigenvalues. From these facts, the system (6) is proven to be stable. □

From Proposition 2, ODE-MMSE method has the following property.

Proposition 3: ODE-MMSE method minimizes the objective function (3).

Proof: The equilibrium point $\boldsymbol{x}^*$ is the unique point for minimizing the objective function (3) where the derivative equals zero. From Proposition 2, the estimate of the ODE-MMSE method is guaranteed to converge to the equilibrium point, i.e., the minimum value. Therefore, the estimate of ODE-MMSE method converges to the unique point for minimizing the objective function. □

The ODE (4) has a close relation to the complex-valued NN [9]. This NN can be regarded as a signal detection system for MIMO by using the transmitted and received signals as the outputs and inputs of the NN, respectively. Moreover, the elementwise equation of (4) has the same formulation as an output of the complex-valued NN which is represented by weighted sum of the complex inputs and bias. This relation motivates the realization of the proposed ODE-MMSE method as well as the complex-valued NN.

IV. MSE ANALYSIS

In this section, we derive an analytical MSE formula and then verify the validity and the convergence property of the ODE-MMSE method by computer simulation.

A. Derivation of Analytical MSE

The MSE between the estimate $\boldsymbol{x}(t)$ and the transmitted signal $\boldsymbol{s}$,

$$\mathrm{MSE}(t) := \mathbb{E}[\|\boldsymbol{x}(t) - \boldsymbol{s}\|^2], \qquad (8)$$

is a principal performance indicator of MIMO signal detection methods [15] but the analytical formula cannot always be derived. For instance, in a signal detection method based on approximate message passing, the MSE is analyzed under the assumption of large system limit [16]. However, the proposed method has the advantage that the analytical MSE formula can be described by a closed-form without any constraint on system parameters, which is shown in Theorem 1 below.

In this section, we derive an analytical MSE formula by using eigenvalue decomposition of the Gram matrix $\boldsymbol{H}^{\mathrm{H}}\boldsymbol{H}$. Suppose that the Gram matrix is decomposed as $\boldsymbol{H}^{\mathrm{H}}\boldsymbol{H} = \boldsymbol{U}\mathrm{diag}[\lambda_1, \ldots, \lambda_n]\boldsymbol{U}^{\mathrm{H}}$, where $\boldsymbol{U} \in \mathbb{C}^{m \times m}$ is a unitary matrix and $\lambda_1, \ldots, \lambda_n$ are nonnegative eigenvalues. We assume $\lambda_1 \geq$

$\ldots \geq \lambda_n \geq 0$ for convenience of the subsequent analyses. By using the decomposition, the following theorem holds.

Theorem 1: The analytical MSE for ODE-MMSE method is given by

$$\begin{aligned}
\mathrm{MSE}(t) = &\sum_{i=1}^{n} \frac{\lambda_i(\lambda_i + \eta - 1)^2(\lambda_i + \sigma^2)e^{-2(\lambda_i+\eta)t}}{(\lambda_i + \eta)^2} \\
&- \sum_{i=1}^{n} \frac{2\lambda_i(\lambda_i + \eta - 1)(\eta - \sigma^2)e^{-(\lambda_i+\eta)t}}{(\lambda_i + \eta)^2} \\
&+ \sum_{i=1}^{n} \frac{\eta^2 + \sigma^2\lambda_i}{(\lambda_i + \eta)^2}.
\end{aligned} \qquad (9)$$

Proof: Substituting (5) for the right-hand side of (8) yields

$$\begin{aligned}
\mathrm{MSE}(t) &= \mathbb{E}\left[\| ((\boldsymbol{Q}(t) + \boldsymbol{R})\boldsymbol{H} - \boldsymbol{I})\,\boldsymbol{s} + (\boldsymbol{Q}(t) + \boldsymbol{R})\,\boldsymbol{w}\|^2\right] \\
&= \mathrm{Tr}\left[((\boldsymbol{Q}(t) + \boldsymbol{R})\boldsymbol{H} - \boldsymbol{I})^{\mathrm{H}}((\boldsymbol{Q}(t) + \boldsymbol{R})\boldsymbol{H} - \boldsymbol{I})\right] \\
&\quad + \sigma^2\mathrm{Tr}\left[(\boldsymbol{Q}(t) + \boldsymbol{R})^{\mathrm{H}}(\boldsymbol{Q}(t) + \boldsymbol{R})\right].
\end{aligned} \qquad (10)$$

The matrix exponential $e^{-(\boldsymbol{H}^{\mathrm{H}}\boldsymbol{H}+\eta\boldsymbol{I})t}$ in $\boldsymbol{Q}(t)$ can be diagonalized by using the eigenvalues of the Gram matrix as

$$e^{-(\boldsymbol{H}^{\mathrm{H}}\boldsymbol{H}+\eta\boldsymbol{I})t} = \boldsymbol{U}\mathrm{diag}[e^{-(\lambda_1+\eta)t}, \ldots, e^{-(\lambda_n+\eta)t}]\boldsymbol{U}^{\mathrm{H}}. \quad (11)$$

From the fact, the terms in (10) can be diagonalized and calculated as

$$\begin{aligned}
&\mathrm{Tr}[(\boldsymbol{Q}(t) + \boldsymbol{R})^{\mathrm{H}}(\boldsymbol{Q}(t) + \boldsymbol{R})] \\
&= \sum_{i=1}^{n} \frac{\lambda_i\left((\lambda_i + \eta - 1)e^{-(\lambda_i+\eta)t} + 1\right)^2}{(\lambda_i + \eta)^2}
\end{aligned} \qquad (12)$$

and

$$\begin{aligned}
&\mathrm{Tr}\left[((\boldsymbol{Q}(t) + \boldsymbol{R})\boldsymbol{H} - \boldsymbol{I})^{\mathrm{H}}((\boldsymbol{Q}(t) + \boldsymbol{R})\boldsymbol{H} - \boldsymbol{I})\right] \\
&= \sum_{i=1}^{n} \frac{\left(\lambda_i(\lambda_i + \eta - 1)e^{-(\lambda_i+\eta)t} - \eta\right)^2}{(\lambda_i + \eta)^2},
\end{aligned} \qquad (13)$$

respectively. The detailed calculation is shown in Appendix. The analytical formula (9) is obtained by summarizing the terms of the matrix exponential. □

Theorem 1 explicitly gives the analytical MSE value of ODE-MMSE method at any time $t \geq 0$. By using this formula, we can describe an asymptotic MSE value, i.e., $\mathrm{MSE}(t)$ at the asymptotic limit of t. Before that, we mention the MSE of MMSE estimation (2) to derive the asymptotic MSE value.

Lemma 1: The MSE of MMSE estimation (2), $\mathrm{MSE}_{\mathrm{mmse}} := \mathbb{E}[\|\hat{\boldsymbol{s}} - \boldsymbol{s}\|^2]$, is given by

$$\mathrm{MSE}_{\mathrm{mmse}} = \sum_{i=1}^{n} \frac{\sigma^2}{\lambda_i + \sigma^2}. \qquad (14)$$

Proof: This can be derived by using MMSE estimate (2) and the eigenvalue decomposition of the Gram matrix. □

Lemma 2: The asymptotic MSE value for ODE-MMSE method, $\mathrm{MSE}_\infty := \lim_{t\to\infty}\mathrm{MSE}(t)$, is given by

$$\mathrm{MSE}_\infty = \sum_{i=1}^{n} \frac{\eta^2 + \sigma^2\lambda_i}{(\lambda_i + \eta)^2}. \qquad (15)$$

The inequality $\mathrm{MSE}_{\mathrm{mmse}} \le \mathrm{MSE}_\infty$ holds and the equality holds if and only if $\eta = \sigma^2$.

Proof: In the case of $t \to \infty$, the first and second terms of (9) vanish because $\lambda_i \ge 0$ for $i = 1, \ldots, n$ and $\eta > 0$. The remaining term is the asymptotic MSE value. The latter statement is supported by the difference between (15) and (14)

$$\mathrm{MSE}_\infty - \mathrm{MSE}_{\mathrm{mmse}} = \sum_{i=1}^{n} \frac{\lambda_i (\eta - \sigma^2)^2}{(\lambda_i + \eta)^2 (\lambda_i + \sigma^2)}$$

is always nonnegative and equals 0 if and only if $\eta = \sigma^2$. $\square$

From Theorem 1 and Lemma 2, we can find that the regularization parameter η controls the convergence rate and the asymptotic MSE value of the ODE-MMSE method. The convergence rate largely depends on behavior of the exponential terms in (9). The larger η accelerates the decrease in the exponential terms, but the asymptotic MSE value could be large depending on the value of η.

B. Numerical Examples

We show numerical examples to confirm validity of the analytical MSE formula (9) and to evaluate the influence of the parameter η on the convergence rate and the asymptotic MSE value (15).

First, we evaluated the validity of the analytical MSE formula (9) by comparing with the arithmetic MSE obtained by Monte Carlo simulation under the single realization of the channel matrix $\boldsymbol{H}$. Each element of the channel matrix $\boldsymbol{H}$ was generated by independent and identical distribution $\mathcal{CN}(0, 1)$. The system parameters were set to $(n, m, \sigma^2, \eta) = (8, 8, 1, 0.5)$. The horizontal line indicates the asymptotic MSE (15). We employed the Euler method, where the behavior of $\boldsymbol{x}(t)$ can be determined directly by the ODE (4) and the estimate at time $t_N = \delta N$, where δ is step-size and $N = 1, 2, \ldots$, is given by

$$\boldsymbol{x}_N = \boldsymbol{x}_{N-1} - \delta(\boldsymbol{H}^\mathrm{H}\boldsymbol{H} + \eta\boldsymbol{I})\boldsymbol{x}_{N-1} + \delta\boldsymbol{H}^\mathrm{H}\boldsymbol{y}. \quad (16)$$

We set $\delta = 10^{-3}$. For the Monte Carlo simulation, pairs of $(\boldsymbol{s}, \boldsymbol{w})$ and the corresponding received signal $\boldsymbol{y}$ were generated 1000 times and the arithmetic MSE was computed. Fig. 1 shows the analytical MSE values of ODE-MMSE method, the arithmetic MSE values of the Euler method, and the asymptotic MSE value of ODE-MMSE method. The curve of the analytical MSE formula is comparable to that of the Euler method with sufficient accuracy. The analytical MSE value converges to the asymptotic MSE value. The results strongly support the validity of the derivation of those theoretical results presented in Sect. IV-A.

Second, we evaluated the influence of the regularization parameter η on the convergence behavior of ODE-MMSE method. Specifically, we focused on the transitional behavior of ODE-MMSE method. The system parameters were set to $(n, m, \sigma^2) = (32, 32, 1)$. Fig. 2 shows the analytical MSE values with $\eta = 0.05, \sigma^2$, and 10. The MSE with $\eta = 10$ rapidly decreases but increases in the middle and finally show the higher asymptotic MSE value at the steady-state. The result
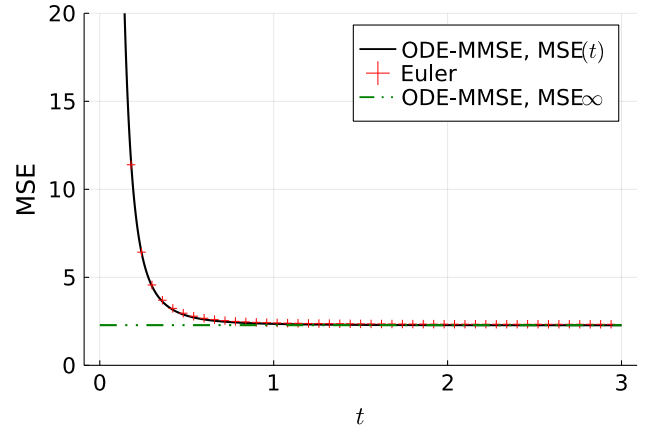

Fig. 1. Comparison of analytical MSE of ODE-MMSE with the arithmetic MSE of the Euler method, $(n, m, \sigma^2, \eta) = (8, 8, 1, 0.5)$.
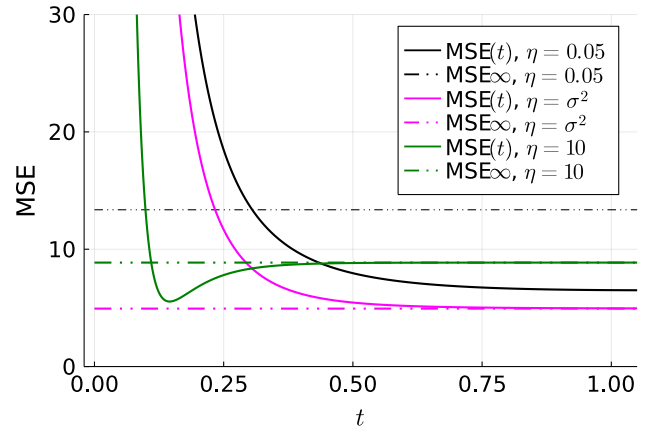

Fig. 2. Comparison of analytical MSE with different choices of the regularization parameter η, $(n, m, \sigma^2) = (32, 32, 1)$.

is consistent with the interpretation of (9) where larger η accelerates decay of the exponential terms. On the other hand, the decrease of the MSE with $\eta = 0.05$ is the slowest but the MSE is lower in $0.5 < t < 1$ than that of $\eta = 10$. The asymptotic MSE is, however, the highest. From these results, the convergence behavior largely depends on the choice of the regularization parameter η and the superiority and inferiority of the MSE values can be switched depending on the time of interest.

V. TIME-DEPENDENT CONTROL OF REGULARIZATION PARAMETER

This section introduces time-dependent control of the regularization parameter aiming at the improvement of the convergence property of ODE-MMSE method.

A. Derivation of Analytical MSE

By the theoretical and simulation results in the previous section, we found that the regularization parameter η significantly affects the convergence property of ODE-MMSE method. Theorem 1 and Fig. 2 indicate that the larger η yields faster convergence of ODE-MMSE method but yields

the worse MSE value than the MMSE estimation (MSE_∞ with $\eta = \sigma^2$). From these results, an adoption of time-dependent control of the regularization parameter η is expected to hold both properties of faster convergence and the better asymptotic MSE value. In this section, we improve ODE-MMSE method to be more flexible by employing the time-dependent regularization parameter $\eta(t)$.

We consider an estimate of s that evolves according to the following ODE

$$\frac{d\boldsymbol{x}(t)}{dt} = -(\boldsymbol{H}^{\mathrm{H}}\boldsymbol{H} + \eta(t)\boldsymbol{I})\boldsymbol{x}(t) + \boldsymbol{H}^{\mathrm{H}}\boldsymbol{y}. \quad (17)$$

The expression $\eta(t)$ implies that the regularization parameter can vary depending on time t. The initial condition is the same as that in (4), i.e., $\boldsymbol{x}(0) = \boldsymbol{H}^{\mathrm{H}}\boldsymbol{y}$. We name the proposed signal detection based on the ODE (17) ODE-MMSE with time-dependent regularization parameter (tODE-MMSE) method.

The ODE (17) can be solved by using variation of parameters method [14] because the matrix $\boldsymbol{A}(t) := \boldsymbol{H}^{\mathrm{H}}\boldsymbol{H} + \eta(t)\boldsymbol{I}$ is commutative.

Proposition 4: The estimate of tODE-MMSE method at time $t \geq 0$ that follows the ODE (17) is given by

$$\boldsymbol{x}(t) = \exp\left(-\boldsymbol{H}^{\mathrm{H}}\boldsymbol{H}t - \xi(t)\boldsymbol{I}\right)$$
$$\times \left(\boldsymbol{I} + \int_0^t e^{\boldsymbol{H}^{\mathrm{H}}\boldsymbol{H}u + \xi(u)\boldsymbol{I}}du\right)\boldsymbol{H}^{\mathrm{H}}\boldsymbol{y}, \quad (18)$$

where $\xi(T) := \int_0^T \eta(s)ds$.

Even in this case, an analytical MSE formula for (18) can be derived in the same way as in Sect. IV-A.

Theorem 2: The analytical MSE for the tODE-MMSE method is given by

$$\text{MSE}(t) = \sum_{i=1}^n \lambda_i(\lambda_i + \sigma^2)\left(1 + \int_0^t e^{\lambda_i u + \xi(u)}du\right)^2 e^{-2(\lambda_i t + \xi(t))}$$
$$- 2\sum_{i=1}^n \lambda_i\left(1 + \int_0^t e^{\lambda_i u + \xi(u)}du\right)e^{-(\lambda_i t + \xi(t))} + n. \quad (19)$$

Proof: MSE can be derived in the same procedure for Theorem 1 by using the eigenvalue decomposition of the Gram matrix. Note that $\xi(t)$ is a scalar and that an integral in terms of a matrix is applied elementwise. □

We can obtain the result of Theorem 1 by setting $\eta(t) = \eta$. The analytical formula (19) has a complicated form, but, like the case of the ODE-MMSE method, the form of time-dependent function $\eta(t)$ influences behavior of the estimation.

B. Numerical Examples

We show numerical examples to confirm validity of the analytical MSE formula (19) and to compare the convergence performance of tODE-MMSE method with that of ODE-MMSE method.

The integral $\xi(t) = \int_0^t \eta(s)ds$ is analytically tractable in some cases. For convenience, we use the following parametric model as the function $\eta(t)$,

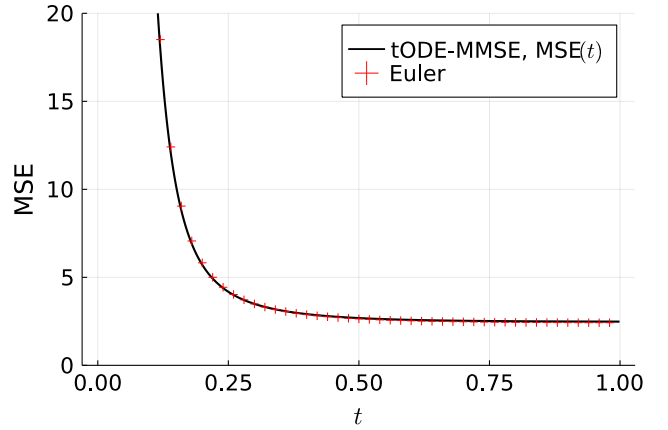$$\eta(t) = \frac{1}{\alpha t + \epsilon} + \sigma^2, \quad (20)$$

Fig. 3. Comparison of analytical MSE of tODE-MMSE with the arithmetic MSE of Euler method, $(n, m, \sigma^2) = (8, 8, 1)$.

where α is a parameter, and ϵ is a small number fixed to 10^{-8} in this paper. The integral can be calculated as $\xi(t) = \frac{1}{\alpha} \log\left(\frac{\alpha t + \epsilon}{\epsilon}\right) + \sigma^2 t$. The function $\eta(t)$ converges to σ^2 at the limit of $t \to \infty$.

We evaluated the validity of the analytical MSE formula (19) by the comparison with the arithmetic MSE obtained by Monte Carlo simulation under the single realization of the channel matrix $\boldsymbol{H}$. We employed the Euler method where η in the equation (16) was replaced with $\eta(t_N)$. The received and transmitted signals and the channel matrix were generated in the same way as in Sect. IV-B. We used the tractable regularization function (20) with $\alpha = 500$. The system parameters were set to $(n, m, \sigma^2) = (8, 8, 1)$. Fig. 3 shows the MSE values at time t of the methods. The curve of the analytical MSE formula is comparable to that of the Euler method, so that the validity of the analytical formula (19) is supported.

Finally, we present an example of using the analytical MSE formula (19) of tODE-MMSE method for improving the convergence property and compare the performance with that of ODE-MMSE method. We have found in Fig. 2 that the performance of the proposed method largely depends on the choice of the regularization parameter. It is expected that we can improve the convergence property by tODE-MMSE method with an appropiate choice of the function $\eta(t)$. There are various possible indicators to evaluate the goodness of convergence performance. In this paper, we employed the functional

$$F(\xi(t)) := \int_0^T \text{MSE}(t)dt$$

as the indicator. If a method holds both properties of faster convergence and lower error, the value of the functional becomes smaller. In the following, we optimize the parameter by minimizing the functional value. Specifically, we choose the parameter that minimizes the functional by employing the grid search.

We set $\alpha = 1, 10, 50, 100$ as the candidates for the parameter. The system parameters were set to $(n, m, \sigma^2) = (8, 8, 1)$

TABLE I
VALUES OF FUNCTIONAL $F(\alpha)$.

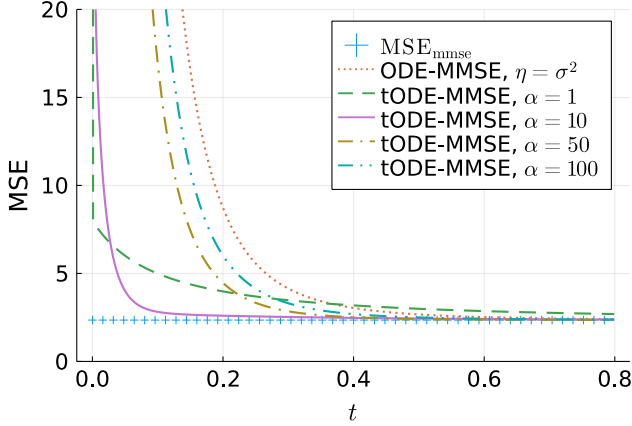| α	1	10	50	100
$F(\alpha)$	2.9136	2.4127	12.4011	17.5674

Fig. 4. The analytical MSE curves with different values of α, $(n, m, \sigma^2) = (8, 8, 1)$.

and $T = 0.8$. Table I summarizes the evaluated values of $F(\xi(t)) = F(\alpha)$. From the table, the value became the lowest with $\alpha = 10$. Fig. 4 shows the MSE of MMSE estimate MSE_{mmse}, the analytical MSE values of ODE-MMSE method with $\eta = \sigma^2$, and those of tODE-MMSE method with different values of α. From the figure, all the MSE curves of tODE-MMSE method converge to the value of MSE_{mmse} faster than ODE-MMSE method. Moreover, the convergence of the method with $\alpha = 10$, which shows the lowest functional value in Table I, is the fastest among the candidates. This indicates that we can find an improved estimation method by the grid search using the functional value.

VI. Conclusions

Analog computing and continuous-time processing are gaining attention from the perspective of computational efficiency of DL and can be solutions to computational load problems in the next generation wireless communication systems. Inspired by this background, we have considered continuous-time MMSE signal detection methods for MIMO systems. We derived the continuous-time estimate as ODE and proposed ODE-MMSE method. The analytical MSE formula is tractable by using eigenvalue decomposition of the Gram matrix of the channel matrix. Simulation results showed the validity of the analytical MSE formula and the significant influence of the choice of the parameter η on the convergence performance. Moreover, we extended the ODE-MMSE method by introducing time-dependent parameter $\eta(t)$ and proposed tODE-MMSE method. The validity of the analytical MSE formula for tODE-MMSE method and its convergence property were confirmed via computer simulation.

As a further development of this research, we can consider deriving a novel discrete-time algorithm by discretization of

an evolution described by ODE. The approach in [11] for obtaining output at any discrete time of NN from ODE can be applied to the development of signal detection algorithms. The novel discrete-time signal detection algorithm is expected to be derived by considering ODE for signal detection.

Appendix

A. Derivation of Theorem 1

The matrix $\boldsymbol{B}(t) := \boldsymbol{Q}(t) + \boldsymbol{R}$ can be calculated as

$$\boldsymbol{B}(t) = \left(\exp\left(-(\boldsymbol{H}^{\mathrm{H}}\boldsymbol{H} + \eta\boldsymbol{I})t\right) \left(\boldsymbol{I} - (\boldsymbol{H}^{\mathrm{H}}\boldsymbol{H} + \eta\boldsymbol{I})^{-1}\right) \right.$$
$$\left. + (\boldsymbol{H}^{\mathrm{H}}\boldsymbol{H} + \eta\boldsymbol{I})^{-1} \right) \boldsymbol{H}^{\mathrm{H}} \tag{21}$$
$$= \boldsymbol{U}\left(\mathrm{diag}\left[e^{-(\lambda_1+\eta)t}\left(1 - \frac{1}{\lambda_1 + \eta}\right), \dots, \right.\right.$$
$$\left. e^{-(\lambda_n+\eta)t}\left(1 - \frac{1}{\lambda_n + \eta}\right)\right]$$
$$\left. + \mathrm{diag}\left[\frac{1}{\lambda_1 + \eta}, \dots, \frac{1}{\lambda_n + \eta}\right]\right) \boldsymbol{U}^{\mathrm{H}}\boldsymbol{H} \tag{22}$$
$$= \boldsymbol{U} \mathrm{diag}\left[\frac{e^{-(\lambda_1+\eta)t}(\lambda_1 + \eta - 1) + 1}{\lambda_1 + \eta}, \dots, \right.$$
$$\left. \frac{e^{-(\lambda_n+\eta)t}(\lambda_n + \eta - 1) + 1}{\lambda_n + \eta}\right] \boldsymbol{U}^{\mathrm{H}}\boldsymbol{H} \tag{23}$$

From (10),

$$\mathrm{Tr}\left[((\boldsymbol{Q}(t) + \boldsymbol{R})\boldsymbol{H} - \boldsymbol{I})^{\mathrm{H}}((\boldsymbol{Q}(t) + \boldsymbol{R})\boldsymbol{H} - \boldsymbol{I})\right]$$
$$= \mathrm{Tr}\left[\mathrm{diag}\left[\left(\left(\frac{e^{-(\lambda_1+\eta)t}(\lambda_1 + \eta - 1) + 1}{\lambda_1 + \eta}\right)\lambda_1 - 1\right)^2, \dots,\right.\right.$$
$$\left.\left.\left(\left(\frac{e^{-(\lambda_n+\eta)t}(\lambda_n + \eta - 1) + 1}{\lambda_n + \eta}\right)\lambda_n - 1\right)\right]\right] \tag{24}$$
$$= \sum_{i=1}^{n} \frac{\left(\lambda_i(\lambda_i + \eta - 1)e^{-(\lambda_i+\eta)t} - \eta\right)^2}{(\lambda_i + \eta)^2} \tag{25}$$

and

$$\mathrm{Tr}[(\boldsymbol{Q}(t) + \boldsymbol{R})^{\mathrm{H}}(\boldsymbol{Q}(t) + \boldsymbol{R})]$$
$$= \mathrm{Tr}\left[\mathrm{diag}\left[\left(\frac{e^{-(\lambda_1+\eta)t}(\lambda_1 + \eta - 1) + 1}{\lambda_1 + \eta}\right)^2 \lambda_1, \dots,\right.\right.$$
$$\left.\left.\left(\frac{e^{-(\lambda_n+\eta)t}(\lambda_n + \eta - 1) + 1}{\lambda_n + \eta}\right)^2 \lambda_n\right]\right] \tag{26}$$
$$= \sum_{i=1}^{n} \frac{\lambda_i\left((\lambda_i + \eta - 1)e^{-(\lambda_i+\eta)t} + 1\right)^2}{(\lambda_i + \eta)^2}. \tag{27}$$

VII. DERIVATION OF LEMMA 1

$\mathrm{MSE}_{\mathrm{mmse}}$

$$= \mathbb{E}[\| \left(\boldsymbol{H}^{\mathrm{H}}\boldsymbol{H} + \sigma^2 \boldsymbol{I} \right)^{-1} \boldsymbol{H}^{\mathrm{H}}(\boldsymbol{H}\boldsymbol{s} + \boldsymbol{w}) - \boldsymbol{s}\|^2] \quad (28)$$

$$= \mathbb{E}\left[\left\| \left(\left(\boldsymbol{H}^{\mathrm{H}}\boldsymbol{H} + \sigma^2 \boldsymbol{I} \right)^{-1} \boldsymbol{H}^{\mathrm{H}}\boldsymbol{H} - \boldsymbol{I} \right) \boldsymbol{s} \right.\right.$$

$$\left.\left. + \left(\boldsymbol{H}^{\mathrm{H}}\boldsymbol{H} + \sigma^2 \boldsymbol{I} \right)^{-1} \boldsymbol{H}^{\mathrm{H}}\boldsymbol{w} \right\|^2 \right] \quad (29)$$

$$= \mathrm{Tr}\left[\left(\left(\boldsymbol{H}^{\mathrm{H}}\boldsymbol{H} + \sigma^2 \boldsymbol{I} \right)^{-1} \boldsymbol{H}^{\mathrm{H}}\boldsymbol{H} - \boldsymbol{I} \right)^{\mathrm{H}} \right.$$

$$\left. \cdot \left(\left(\boldsymbol{H}^{\mathrm{H}}\boldsymbol{H} + \sigma^2 \boldsymbol{I} \right)^{-1} \boldsymbol{H}^{\mathrm{H}}\boldsymbol{H} - \boldsymbol{I} \right) \right]$$

$$+ \sigma^2 \mathrm{Tr}\left[\left(\left(\boldsymbol{H}^{\mathrm{H}}\boldsymbol{H} + \sigma^2 \boldsymbol{I} \right)^{-1} \boldsymbol{H}^{\mathrm{H}} \right)^{\mathrm{H}} \right.$$

$$\left. \cdot \left(\left(\boldsymbol{H}^{\mathrm{H}}\boldsymbol{H} + \sigma^2 \boldsymbol{I} \right)^{-1} \boldsymbol{H}^{\mathrm{H}} \right) \right] \quad (30)$$

$$= \sum_{i=1}^{n} \left(\frac{\lambda_i}{\lambda_i + \sigma^2} - 1 \right)^2 + \sigma^2 \sum_{i=1}^{n} \left(\frac{\lambda_i}{(\lambda_i + \sigma^2)^2} \right) \quad (31)$$

$$= \sum_{i=1}^{n} \frac{\sigma^2}{\lambda_i + \sigma^2} \quad (32)$$

VIII. DERIVATION OF THEOREM 2

The matrix in (18) can be decomposed as

$$\exp\left(-\boldsymbol{H}^{\mathrm{H}}\boldsymbol{H}t - \xi(t)\boldsymbol{I} \right) \left(\boldsymbol{I} + \int_0^t e^{\boldsymbol{H}^{\mathrm{H}}\boldsymbol{H}u + \xi(u)\boldsymbol{I}} du \right)$$

$$= \boldsymbol{U}\left(\mathrm{diag}\left[e^{-(\lambda_1 t + \xi(t))} \left(1 + \int_0^t e^{\lambda_1 u + \xi(u)} du \right), \ldots, \right.\right.$$

$$\left.\left. e^{-(\lambda_n t + \xi(t))} \left(1 + \int_0^t e^{\lambda_n u + \xi(u)} du \right) \right] \right) \boldsymbol{U}^{\mathrm{H}}. \quad (33)$$

By using this, the analytical MSE can be derived in the same way as Theorem 1.

REFERENCES

[1] E. C. Strinati, D. Belot, A. Falempin, and J.-B. Doré, "Toward 6G: From new hardware design to wireless semantic and goal-oriented communication paradigms," in Proc. ESSCIRC, Grenoble, France, Sept. 2021, pp. 275–282.

[2] K. Li, R. Sharan, Y. Chen, T. Goldstein, J. R. Cavallaro, and C. Studer, "Decentralized baseband processing for massive MU-MIMO systems," IEEE J. Emerg. Sel. top. Circuits Syst., vol. 7, no. 4, pp. 491–507, Dec. 2017.

[3] N. Kim, Y. Lee, and H. Park, "Performance analysis of MIMO system with linear MMSE receiver," IEEE Trans. Wireless Commun., vol. 7, no. 11, pp. 4474–4478, Nov. 2008.

[4] S. Chetan, J. Manikandan, V. Lekshmi, and S. Sudhakar, "Hardware implementation of floating point matrix inversion modules on FPGAs," in Proc. ICM, Aqaba, Jordan, Dec. 2020, pp. 1–4.

[5] J. Welser, J. W. Pitera, C. Goldberg, "Future computing hardware for AI," in Proc. IEDM, San Francisco, CA, USA, Dec. 2018.

[6] W. Haensch, T. Gokmen, and R. Puri, "The next generation of deep learning hardware: Analog computing," Proc. IEEE, vol. 107, no. 1, pp. 108–122, Jan. 2019.

[7] E. A. Cartier, W. Kim, N. Gong et al., "Reliability challenges with materials for analog computing," in Proc. IRPS, Monterey, CA, USA, Mar.–Apr. 2019.

[8] X. Lin, Y. Rivenson, N. T. Yardimci, M. Veli, Y. Luo, M. Jarrahi, and A. Ozcan, "All-optical machine learning using diffractive deep neural networks," Science, vol. 361, no. 6406, pp. 1004–1008, Jul. 2018.

[9] H. Zhang, M. Gu, X. D. Jiang et al., "An optical neural chip for implementing complex-valued neural network," Nat. Commun., vol. 12, no. 457, pp. 1–11, Jan. 2021.

[10] S. Abdollahramezani, O. Hemmatyar, and A. Adibi, "Meta-optics for spatial optical analog computing," Nanophotonics, vol. 9, no. 13, pp. 4075–4095, Sept. 2020.

[11] R. T. Q. Chen, Y. Rubanova, J. Bettencourt, and D. K. Duvenaud, "Neural ordinary differential equaitons," in Proc. NeurIPS, Montréal, Canada, Dec. 2018, pp. 1–13.

[12] Y. Zhang, "Revisit the analog computer and gradient-based neural system for matrix inversion," in Proc. ISIC, Limassol, Cyprus, Jun. 2005, pp. 1411–1416.

[13] K. Li, O. Castañeda, C. Jeon, J. R. Cavallaro, C. Studer, "Decentralized coordinate-descent data detection and precoding for massive MU-MIMO," in Proc. ISCAS, Sapporo, Japan, May 2019.

[14] G. Teschl, Ordinary differential equations and dynamical systems, vol. 140, American Mathematical Soc., 2012.

[15] M. Joham, W. Utschick, and J. A. Nossek, "Linear transmit processing in MIMO communications systems," IEEE Trans. Signal Process., vol. 53, no. 8, pp. 2700–2712, Aug. 2005.

[16] R. Hayakawa and K. Hayashi, "Discreteness-aware approximate message passing for discrete-valued vector reconstruction," IEEE Trans. Signal Process., vol. 66, no. 24, pp. 6443–6457, Dec. 2018.